Available online at www.sciencedirect.com
SCIENCE DIRECT®
Microporous and Mesoporous Materials 72 (2004) 227–238
MICROPOROUS AND MESOPOROUS MATERIALS
www.elsevier.com/locate/micromeso

Influence of residual cations (Na^+, K^+ and Mg^{2+}) in the alkylation activity of benzene with 1-octene over rare earth metal ion exchanged FAU–Y zeolite

Bejoy Thomas, S. Sugunan *

Department of Applied Chemistry, Cochin University of Science and Technology, Kochi, Kerala 682 022, India

Received 31 August 2003; received in revised form 8 April 2004; accepted 12 April 2004

Abstract

The effect of residual cations in rare earth metal modified faujasite–Y zeolite has been monitored using magic angle spinning NMR spectral analysis and catalytic activity studies. The second metal ions being used are Na^+, K^+ and Mg^+. From a comparison of the spectra of different samples, it is concluded that potassium and magnesium exchange causes a greater downfield shift in the ^{29}Si NMR peaks. Also, lanthanum exchanged samples show migration behavior from large cages to small cages, which causes the redistribution of second counter cations. It is also observed that Mg^{2+} causes the most effective migration of lanthanum ions due to its greater charge. The prepared systems were effectively employed for the alkylation of benzene with 1-octene in the vapor phase. From the deactivation studies it is observed that the as-exchanged zeolites possess better stability towards reaction condition over the pure HFAU zeolite.

Keywords: Rare earth exchanged faujasite–Y zeolite; Magic angle spinning NMR; Hirschler–Plank mechanism; Migration behavior; Linear alkylation benzene; 2-Phenyloctane; Deactivation studies

1. Introduction

The rare earth exchanged forms of zeolite–Y exhibit high thermal stability, acidity and have been extensively used in petroleum-refining processes. Lanthanum exchanged faujasite–Y zeolite is an important fluid catalytic cracking catalyst in the hydrocracking of heavy petroleum products [1,2]. Various rare earth exchanged faujasite–Y zeolites are used for the synthesis of linear alkyl benzenes, which forms the basic components for the manufacture of commercial detergents [3,4]. Acidity and thermal stability of synthetic Na–Y can be improved by ion exchanging with rare earth metal ions and the extent of improvement is controlled by the degree of exchange and therefore the location of cations. The structural characteristics and catalytic applications of various rare earth substituted Na–Y have been investigated; most of the published studies were on lanthanum and cerium exchanged Na–Y zeolites [5,6].

Modern techniques of solid state NMR spectroscopy such as MAS, DOR and two dimensional nutation and multiple quantum NMR spectroscopy were applied to separate signals of sodium cations located at different cation positions in dehydrated zeolite–Y [7,8]. The quantitative evaluation of ^{23}Na MAS NMR spectra allows one to determine the population of different cation sites. Welsh and Lambert [9] observed two lines in the ^{23}Na MAS NMR spectrum; one at −9 ppm which is assigned to sodium cations in the large cavities on cation position SII and non-localized sodium cation in the large cavities. Second one at −13 ppm was assigned to sodium cations located on cation position SI′ in the sodalite cages. However, Bayer et al. [10] attributed the line at −9 ppm to hydrated sodium ions on position SI′ and SII′. A line at −5.5 ppm occasionally observed in the spectra of hydrated lanthanum exchanged faujasite

* Corresponding author. Tel.: +91-484-2575804; fax: +91-484-2577595.
E-mail address: ssg@cusat.ac.in (S. Sugunan).

1387-1811/$ - see front matter © 2004 Published by Elsevier Inc.
doi:10.1016/j.micromeso.2004.04.021

zeolite is ascribed to sodium cations in hexagonal prisms (SI). Challoner and Harris [11] observed line in the static spectra of hydrated Na–Y, which they assumed to be due to the satellite transitions ($\pm 1/2 \leftrightarrow \pm 3/2$) of sodium nuclei undergoing isotropic tumbling.

High resolution solid state ^{29}Si MAS NMR has been used to study the Si, Al ordering in zeolites providing information about the immediate local environment of Si atom. The ^{29}Si peak positions shifts to the low field by an increase in the number of AlO_4 tetrahedra or to the higher field by increasing the average Si–O–Si or Si–O–Al bond angles [12–15]. ^{27}Al is used to study the coordination around Al^{3+}, which is either a tetrahedral or an octahedral species. Hence it is said to be susceptible to the oxygen coordination and strain in the framework AlO_4 tetrahedra [4,14,16].

There have not been many reports on the effect of residual cation on the nuclear magnetic properties of rare earth modified faujasite–Y zeolite. Chao and Chern [15] found that ion exchange of Na–Y zeolite with potassium, calcium, barium, magnesium and strontium cations and subsequent dehydration brings about a high field shift of the Si(nAl) signals, where n is the number of aluminium atoms in the second coordination sphere of the resonating silicon atoms. This high-field shift was explained by the local strain of the framework SiO_4 tetrahedra in the neighborhood of extra-framework positions occupied by large cations.

Many solids acids like metal oxides [17,18] clays [3,19] and zeolites [20–29] have been tested for their ability to alkylate benzene with detergent range of olefins under different experimental conditions. Many of these have activities comparable to those of common liquid acid catalysts such as HF and $AlCl_3$. These are highly corrosive and possess extreme affinity for water, which makes them difficult to handle. Under the reaction conditions these reagents are converted to materials that are toxic and non environmentally friendly. Since the reagents are irreversibly lost, the overall atom efficiency is very low. Although many of these solid acids are active, the lack of selectivity for LAB's and stability to process time are serious problems [30]. A successful solid acid catalyst demands activity, selectivity, reusability and stability towards coking, etc. so as to be economical compared to HF. In this regard, we have prepared the zeolite faujasite H–Y in different rare earth modified forms. Exchange with rare earth metal ions improves the structural and textural properties of the zeolite. The activities of the prepared systems have been checked for the alkylation of benzene with 1-octene under constant flow of nitrogen. High chemical and thermal stability of the systems, high activity, reusability and resistance to deactivation coupled with its eco-friendly nature makes rare earth metal modified zeolites a much better catalyst for the synthesis of LAB's over the conventional catalysts like HF or $AlCl_3$.

2. Materials, methods and experiments

2.1. Catalyst preparation

Binder free sodium, potassium and magnesium exchanged varieties were prepared by ion exchanging the parent H–Y with 0.1 M solution of the respective nitrate at room temperature for 3 times. This was followed by washing with demineralized water, drying at 383 K for over night in an air oven and calcining to 773 K. Rare earth exchanged forms were prepared by ion exchanging Na–Y, K–Y and Mg–Y with a 0.5 M respective nitrate solution at 353 K for 24 h. It was then filtered, washed with de-ionized water followed by drying at 383 K in an air oven for over night. All the samples were then calcined at temperatures from 423 to 773 K, and at 773 K for 5 h with a heating rate of 12 K/min with a constant air blowing over the sample [31,32].

2.2. Catalyst characterization

The percentage of metal ion exchanged and framework Si/Al ratio were determined by EDX using a *JEOL JSM-840 A* (Oxford make model l6211 with a resolution of 1.3 eV). The diffuse reflectance UV–visible spectroscopy was carried out over an *Ocean optics AD 2000* spectrometer (200–900 nm) with CC detector. Structural information was obtained from XRD performed over *Rigaku D-max C* X-ray diffractometer with Ni-filtered Cu Kα radiation and IR performed over a *Nicolet Impact 400FT IR* spectrometer. Surface acidity determination was done using temperature programmed desorption (TPD) of ammonia using a conventional equipment.

Solid-state NMR experiments were carried out over a *Brucker DSX-300* spectrometer at resonance frequencies of 78.19 MHz for ^{27}Al and 59.63 MHz for ^{29}Si and 79.97 MHz for ^{23}Na. For all the experiments a standard 4 mm double-bearing *Brucker* MAS probe was used. A sample rotation frequency of 8 kHz for ^{23}Na, 7 kHz for ^{27}Al, and ^{29}Si with a single pulse excitation corresponding to $\pi/2$ flip angle. The pulse lengths for the experiments were 5.5 μs, 10 μs and 4 μs for ^{23}Na, ^{27}Al and ^{29}Si, respectively, whereas the pulse delays were 0.5, 2, and 5 s.

Activity of the prepared systems was tested for the alkylation of benzene with 1-octene. Reaction was carried out in a fixed-bed, down-flow reactor made of glass with 0.6 cm internal diameter and 30 cm height. Catalysts were activated for 12 h in presence of oxygen, allowed to cool to room temperature in dry nitrogen and then heated to reaction temperature where it was kept for one hour to stabilize. The reactants were fed into the reactor in presence of dry N_2 to provide inert atmosphere. For all the reactions carried out, products were collected at third hour and identification was done using

a *Chemito* 8610 Gas Chromatograph fitted with a FID detector and 20% OV-101 column. Column temperature was adjusted between 383 and 503 K, injector temperature was 503 K and detector temperature was 523 K. Isomer determination was done using a *Shimadzu QP 2010*-GCMS with universal capillary column. The MS detector voltage was 1 kV. The *m/z* values and relative intensity (%) are indicated for the significant peaks. (Column temperature was adjusted between 323 and 533 K with heating rate of 10 K/min, injector: 513 K and detector: 563 K).

3. Results and discussion

Energy dispersive X-ray analysis (EDX) measurements show an overall Si/Al ratio of 1.5 for all the as-exchanged zeolite systems. In all the cases more than 80% of sodium got exchanged with rare earth metal cations. Thermal studies on the samples show that the parent and different as-exchanged systems are highly stable at 873 K. From scanning electron micrographs of the parent and as-exchanged samples, an average idea about the average particle size, which decreases upon exchange with rare earth cations, is obtained.

Diffuse reflectance UV–visible spectroscopy is known to be a sensitive probe for the identification and characterization of metal ion coordination and its existence in the framework and/or in the extra framework position of metal containing zeolites. The position of the metal to ligand charge transfer spectra [$O^{2-} \rightarrow Ce^{4+}$] depends on the ligand field symmetry surrounding the cerium center. Depending on the coordination of the metal ions it shows two absorption bands; one at/or around 300 nm and another around 400 nm. The electronic transition from cerium to oxygen require high energy for the tetra coordinated Ce^{4+} than the hexa coordinated one [33]. Among the different zeolitic samples, only the cerium exchanged one exhibits activity towards UV–visible diffuse reflectance. It shows an intense band around 300 nm. Therefore it may be inferred that the absorption band centered around 300 nm for the CeNa–Y sample is due to the presence of well-dispersed Ce^{4+} in a tetra-coordinated environment. This charge transfer peak is possible due to presence of the flexibility in the oxidation state of cerium, ($Ce^{3+} \leftrightarrow Ce^{4+}$). Other as-exchanged samples do not show CT bands predominantly due to the lack of flexible oxidation states in the metal cation as in the case of cerium. However, in the low energy region they exhibit very small shoulder peaks due to less intense $f \rightarrow f$ transitions. UV–visible DRS confirms the presence only one type of well dispersed cerium species (tetra coordinated).

Vibrational spectra show bands both in the framework and hydroxyl regions (Fig. 1). In the framework

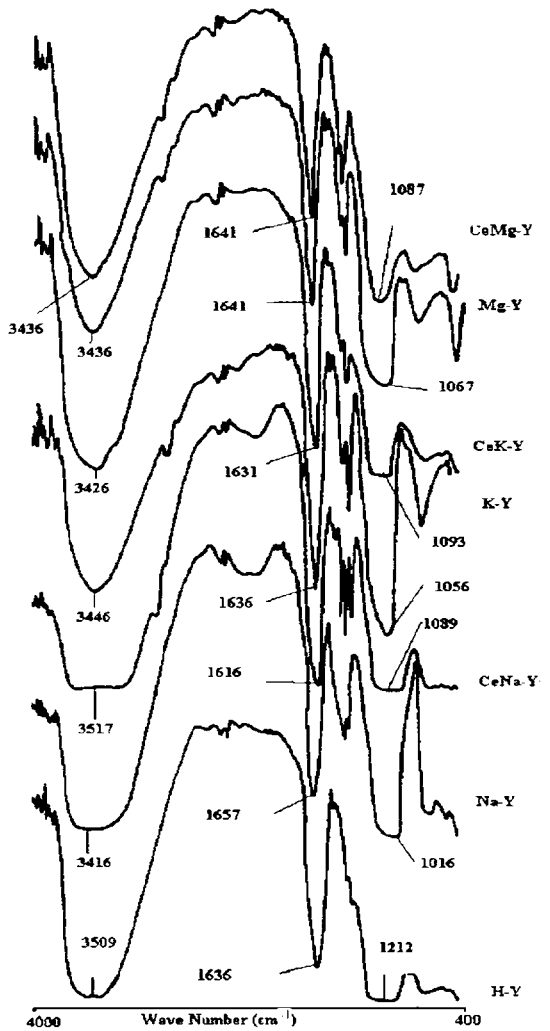

Fig. 1. FT-IR spectra of various parent zeolites H–Y, Na–Y, K–Y and Mg–Y and different as-exchanged cerium zeolites CeNa–Y, CeK–Y and CeMg–Y in the 400–4000 cm^{-1} range recorded in the transmission mode.

region 400–1300 cm^{-1}, we got a very broad band between 900–1100 cm^{-1}, which corresponds to Si–O–Si vibration around 1090 cm^{-1}, Si–O–Ce around 970 cm^{-1} and Si–O stretching vibrations of the $Si-O^{-}-R^{+}$ ($R^{+} = H^{+}$) groups in the calcined state. In the hydroxyl region (3000–4000 cm^{-1}), a broad band is observed around 3450 cm^{-1} in all the samples, which is assigned to ν_{OH} of Si–O–H. Due to the in plane bending $\delta_{OH}(H_2O)$ of hydroxyl groups, a band around 1630 cm^{-1} is observed. Consistent with the earlier reports, XRD analysis confirms crystallization of the parent and modified forms into cubic unit cell withspace group F3dm (Fig. 2). Percentage crystallinity of samples decreases in the order Na–Y > LaNa–Y > CeNa–Y > H–Y. This is due to the decrease in the electropositivity of the counter cation.

As seen in the Table 1, the total amount of ammonia adsorbed by each sample varies with the nature of cation

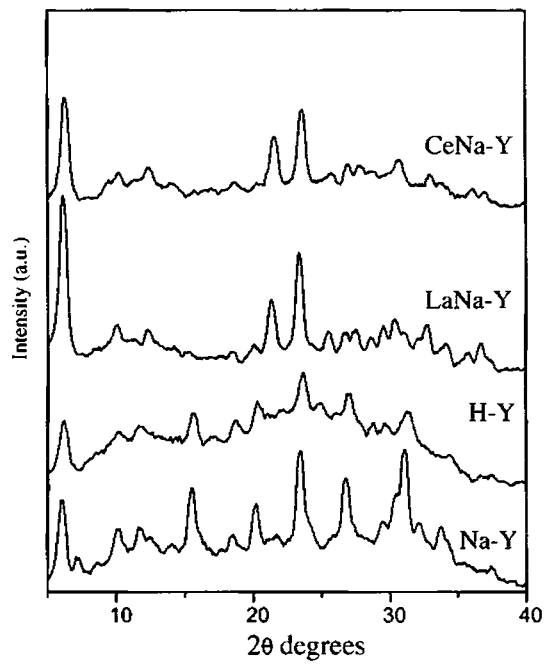

Fig. 2. X-Ray diffraction patterns of representative samples.

present. Irrespective of the cation present, all samples show high values of acidity in the weak and medium regions. Among the samples, CeNa–Y and CeMg–Y shows maximum acidity. As we go from potassium to sodium to magnesium for a fixed rare earth cation the acidity increase. The very specific influence of Mg^{2+} cation in introducing greater acidity in its parent as well as rare earth modified forms is due to its very high polarizing power which affects the OH bond strength through the lattice. Low value in the acidity of LaNa–Y, LaK–Y and LaMg–Y is due to the formation of inaccessible Brönsted acid sites (BASs) in the small cages upon heat treatment. These inaccessible BASs in the small cages are formed by the migration of La^{3+} from super cage to small cages in the electrostatic repulsive field of residual cations. This migration is most in the case of magnesium cation and consequently shows the maximum variation in acidity from the parent form Mg–Y. This observation correlates well with the results from NMR spectral studies and thermodesorption of pyridine and 2,6-dimethyl pyridine.

3.1. NMR studies

^{23}Na NMR spectra of Na–Y and different as-exchanged zeolites calcined at 773 K are shown in Fig. 3. ^{23}Na NMR spectra of dehydrated RE–Y zeolites give three peaks at chemical shift values −13, −31 and −63 ppm. Engelhardt et al. [34] proposed the peak at −13 ppm is due to Na cations located at the center of the hexagonal prisms on position SI or SII of the sodalite cages, which will be a low field Gaussian line (GL). Even at 773 K the Na cations will not be fully dehydrated and the simulation of ^{23}Na NMR spectra of dehydrated samples may have an additional line at −24 ppm, which has been assigned to the incompletely dehydrated Na cations. Na cations located close to the center of six membered ring window on position SI′ and SII show a high field (−61 ppm) quadrapole pattern (QP) with a quadrapole frequency of $\upsilon_q = 2.1$ MHz, an asymmetry parameter of $\eta = 0.25$ and an isotropic chemical shift of −8 ppm[7]. Massoiot et al. [35] identified the contribution of this QP line to the central GL as 16%. The non-localized Na^+ ions in the large cavities of the faujasite are observed at an NMR shift of −9 ppm. The peak at −13 ppm was found to be caused by two components, the component that is characterized by a quadrupolar interaction causing a field depended shift and a signal at $\upsilon = 2\upsilon_{rf}$ in the two dimensional quadrupolar nutation spectra is attributed to Na^+ enclosed in the sodalite cages. All the as exchanged samples exhibit a single peak between −8.95 and −10.57 ppm. The absence of peak at −13 ppm suggest the absence of localized Na^+ ions in the sodalite cages of zeolite framework. The absence of

Table 1
Acid structural properties of different systems studied by temperature desorption of ammonia method

Catalyst systems	Ammonia desorbed			
	Weak mmol/g (373–473 K)[a]	Medium mmol/g (474–673 K)	Strong mmol/g (674–873 K)	Total acidity mmol/g
H–Y	0.41	0.63	0.30	1.34
Na–Y	0.59	0.12	0.05	0.77
CeNa–Y	1.45	0.59	0.20	2.24
LaNa–Y	0.92	0.42	0.13	1.48
K–Y	0.40	0.20	0.09	0.71
CeK–Y	0.62	0.38	0.23	1.23
LaK–Y	0.47	0.35	0.12	0.94
Mg–Y	0.60	0.51	0.18	1.29
CeMg–Y	1.41	0.63	0.24	2.28
LaMg–Y	0.77	0.53	0.11	1.41

[a] The ammonia disorbed in the temperature range 373–473 K might contain small amounts of physisorbed ammonia too.

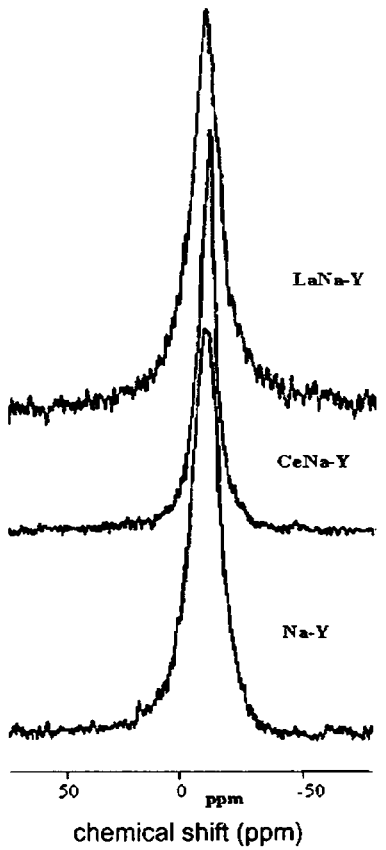

Fig. 3. ^{23}Na MAS NMR spectra of parent Na–Y zeolite and of the as-exchanged zeolites CeNa–Y and LaNa–Y recorded at a resonance frequency of 79.97 MHz with a sample spinning speed of 8 kHz.

peaks at −24 and −61 ppm confirm the nonexistence of incompletely dehydrated Na^+ ion and sodium cation located close to the center of six membered ring window on positions SI and SII. A single peak at or around −9 ppm confirms that all the Na^+ ions in the samples are non-localized. Pure Na–Y shows a chemical shift of −10.57 ppm and all the as-exchanged forms show chemical shifts lower than this. These shifts in the peak positions can be explained by the electrostatic repulsive force between Na^+ ions and other bulky rare earth cations. The shift value of CeNa–Y and LaNa–Y are −10.55 and −8.95 ppm, respectively. Ce^{3+} induced a very small difference in the peak positions from Na–Y (0.02 ppm). The line width at half height, $\Delta\upsilon_{1/2}$, of the MAS spectra of Na–Y, CeNa–Y and LaNa–Y are 1062, 549.32 and 451 Hz, respectively, which is much smaller than the spinning speed of 7 kHz in the MAS NMR experiments. As expected, the sodium-exchanged form exhibits the maximum and the lanthanum the least width at half height. The large value of $\Delta\upsilon_{1/2}$ corresponds to large quadrupole interactions of its sodium nuclei. This increase of line width is probably due to a reduced mobility of either the sodium ions or water molecules in the zeolite. Similar to any other NMR experiments of the same samples, La^{3+} exchanged zeolite–Y shows unusual peak position and $\delta\upsilon_{1/2}$. This rather complicated result could be explained using the migration probabilities of La^{3+} ions from the large sodalite cages to the small cages and preferential formation of Brönsted acidity in presence of more electropositive counter cations. This observation correlates well with the results obtained from ^{27}Al, ^{29}Si and acidity determination experiments like TPD and thermodesorption studies.

The ^{27}Al MAS NMR spectra of calcined samples give rise to only one resonance peak around 60 ppm due to aluminium in a tetrahedral environment, which is typical for zeolitic framework aluminum (Fig. 4a–c). But, some samples show a small peak at 0 ppm, which is due to the extra framework octahedral aluminum formed by leaching during thermal exchange. Absence of peaks around 30 and 80 ppm confirms the lack of penta-coordinated aluminium species and $Al(OH)_4^-$. It has been reported that the ^{27}Al NMR spectroscopy of zeolites is sensitive to the oxygen coordination of aluminium atoms and to the strain of the framework AlO_4 tetrahedra [14]. The appearance of the broad line in the ^{27}Al MAS NMR spectrum is due to strain in the Al–O–T bonds caused by the presence of bulky highly charged cations. This spectral broadening increases in the order of H–Y < Na–Y < K–Y ≅ Mg–Y. A similar observation is seen in the case of rare earth exchanged forms. Broadening is caused by the distribution of chemical shifts due to aluminium atoms in the locality of strained (due to vicinity of heavy or bulky cations) and non-strained framework. Aluminium with spin 5/2 are involved in quadrupolar interaction with electric field gradients caused by the electric changes in the surrounding of the Al nuclei. These electric field gradients are small for symmetric charge distribution, i.e., for fully hydrated and mobile Na, K or Mg cation in the large cavities. But, they are large for non- symmetric charge distribution, e.g. for residual cation located close to the center of six membered oxygen ring, such as position SI′ in the sodalite cages [36]. The greater line width for K and Mg suggests a greater quadrupolar influence and enhanced probability of a residual cation being at or near to the small cage (SI′). Parent H–Y shows a chemical shift of 61.29 ppm. All other as-exchanged zeolite systems exhibits a chemical shift less than this value. This shift in the peak position to high field region is easily be correlated to the strain of the AlO_4 framework.

High resolution solid state ^{29}Si NMR with magic angle spinning (MAS) has been shown to be effective in determining the Si, Al ordering in zeolites, providing direct information of the local environment of silicon atom. ^{29}Si peak positions shift either to lower field or to the higher field according to the nature of the counter cations. This shift can also be due to the change in the Si–O–Si or Si–O–Al bond angles [14,37]. It has been applied for the identification of framework in the

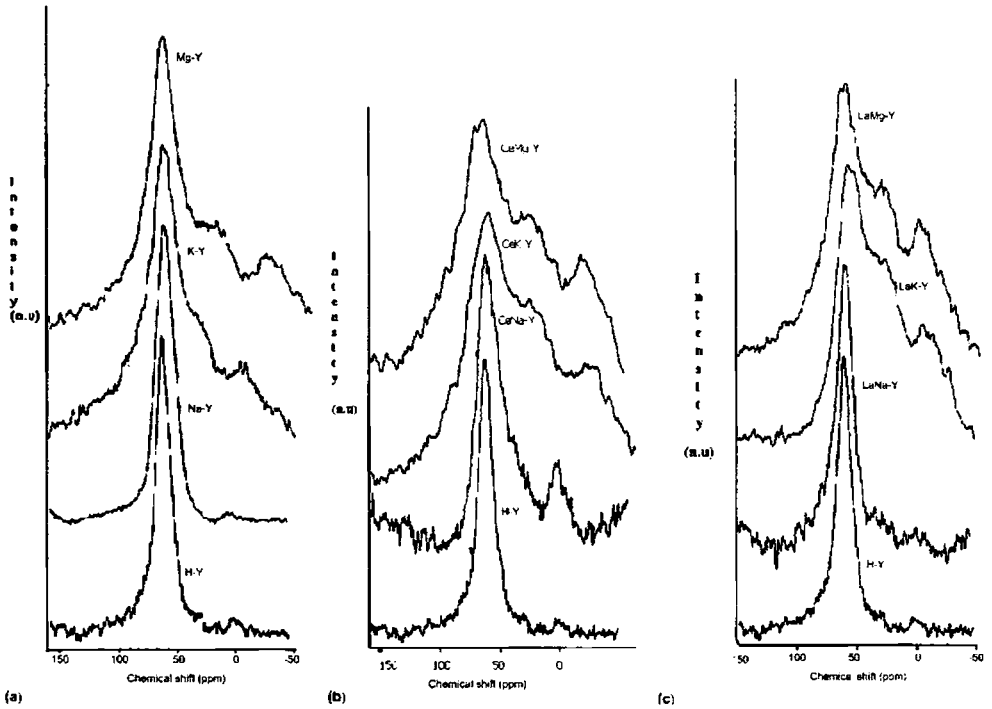

Fig. 4. ^{27}Al MAS NMR spectra of parent zeolites H–Y, Na–Y, K–Y and Mg–Y (a) and of the H–Y zeolite and various cerium exchanged zeolites CeNa–Y, CeK–Y and CeMg–Y (b) as well as H–Y and different lanthanum exchanged zeolites LaNa–Y, LaK–Y and LaMg–Y (c) recorded at a resonance frequency of 78.19 MHz with a sample spinning speed of 7 kHz.

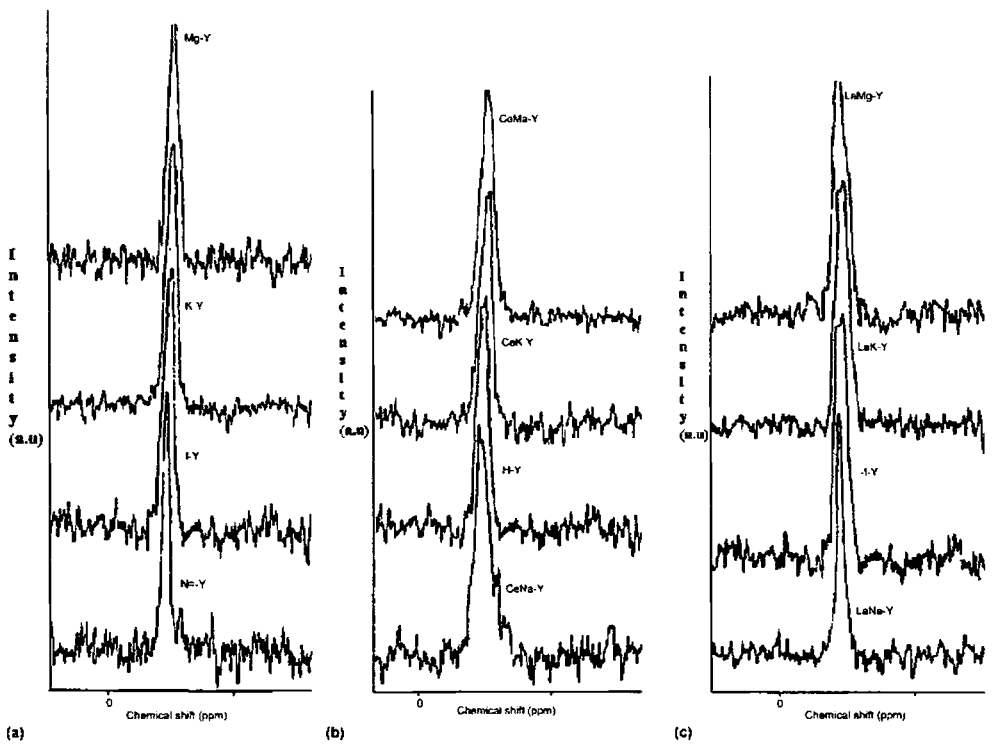

Fig. 5. ^{29}Si MAS NMR spectra of parent zeolites H–Y, Na–Y, K–Y and Mg–Y (a) and of the H–Y zeolite and various cerium exchanged zeolites CeNa–Y, CeK–Y and CeMg–Y (b) as well as H–Y and different lanthanum exchanged zeolites LaNa–Y, LaK–Y plus LaMg–Y (c) recorded at a resonance frequency of 59.63 MHz with a sample spinning speed of 7 kHz.

zeolites. Q-unit is used to indicate the different silicate atoms in the systems. In zeolites, the Q-unit is always Q4, where four silicate or alumina surrounds each silicate units. Generally they are noted as Si(nAl) or Si($4-n$)Si, indicating that each Si atom is linked through oxygen to n aluminium and $4-n$ silicon neighbors [37]. Applying ^{29}Si NMR spectroscopy it was found that the exchange of zeolite Na–Y with lanthanum, cerium, samarium, potassium, calcium, barium and magnesium cations and subsequent dehydration brings about high field shift of Si(nAl) signals, where n is the number of aluminium atoms in the second coordination sphere of the resonating silicon atom [15,38]. Consistent with the observed results K–Y, Mg–Y and K^+ and Mg^{2+} exchanged rare earth zeolites exhibited a high field shift over Na^+ exchanged samples (Fig. 5a–c). The chemical shift values are comparable for the zeolites with K^+ and Mg^{2+} residual cations. This high field shift is due to the local strain of the framework SiO_4 tetrahedra in the neighborhood of extra framework positions occupied by bulky and highly charged residual cations. The main central peak in the as-exchanged CeNa–Y and LaNa–Y shows 3 shoulder peaks which might be originating from Si(nAl) with $n = 3$, 2 and 1 whereas the central peak must be that of Si(OSi)$_4$ unit. Such a clear split could not be observed in the case of other modified forms. The high field shifts in the spectra of the as-exchanged samples and the corresponding cation migration influences the number of bulky cations (La^{3+} and Ce^{3+}) that are accessible for the formation of accessible Brönsted acid sites according to Hirschler–Plank mechanism [39]. During heating and dehydration, the La^{3+} ions (ionic diameter 0.23 nm) strip off their hydration sphere and migrate from supercages into small sodalite or hexagonal prism cavities [12]. Hence the cation distribution in the lanthanum-exchanged forms is a function of heat treatment and the nature of the residual cation. Comparison of chemical shifts values of the as-exchanged samples shows that lanthanum exchanged ones exhibits a lower shift values over the cerium exchanges ones. This is most predominant in the case of Mg form. It is explained as due to the migration of La^{3+} ions in the electrostatic repulsive field of Na^+, K^+ and Mg^{2+} ions. The values show that the Mg^{2+} exert the maximum repulsion on La^{3+} due to its comparatively high charge over K^+ and Na^+. The repulsive interaction of residual ions enhances the migration of lanthanum cations into the small cages.

4. Alkylation of benzene with 1-octene

The carbocation alkylation of arenes with detergent range of linear olefins (see Scheme 1 for reaction mechanism) with protonic acids typically produces mixed phenylalkanes that are positional isomers, i.e., 2-phenyl, 3-phenyl, etc. In the present case of 1-octene, four carbocations are possible and the relative stabilities of them increases towards the center of the chain. So the least stable is the primary ion (1-position) and due to its very low stability, 1-phenyl isomer is not detected in the product.

On the basis of relative stabilities of the other carbocations (all secondary), it is expected that the isomer content increase towards the center of the chain. This is found to be so in the case of HF, in which the thermodynamic equilibrium is probably reached. However, in the case of HFAU–Y, rare earth exchanged zeolite–Y and H-mordenite, the 2-phenyl isomer content is greater suggesting the non-attainment of thermodynamic equilibrium.

In the mechanism prescribed above, a carbocation (2, 3 or 4) is generated by accepting a proton from zeolite (**2**, **3**, etc.). 2-carbocation attack the benzene ring leading to the formation of an intermediate **5**, which eliminates a proton to produce 2-phenyoctane (**6**). In a similar way the interaction of other carbocation isomers produce other phenyloctane isomers (not given). Multiple attacks of the carbocation on the benzene ring leads to the formation of dialkylates and trialkylates. The possible mechanism for the alkene cracking and isomerization are depicted in the remaining part of the scheme. However, these reactions occurred to a limited extent under the given reaction conditions.

The conversion of 1-octene and selectivity for the 2-phenyloctane were calculated according to the method proposed by de Almeida et al. [22]

$$\text{Conversion} = \frac{N_{A0} - N_A}{N_A} \times 100,$$

where, N_{A0} is the initial number of moles of 1-octene and N_A is the number of moles of 1-octene at time t.

$$\text{Selectivity} = \frac{N_n}{N_{A0} - N_A} \times 100,$$

where, N_n is the number of moles of product n.

The total conversion of 1-octene and selectivity for 2-phenyloctane formation have been studied by varying the amount of the catalyst. Fig. 6 shows the dependence of the amount of catalyst on the conversion and selectivity. It is seen that as the amount of catalyst increases from 0.25 to 1.25 g the total conversion increases from 55% to 92.7%. With the increase of catalyst loading the probabilities for reaction over the external surface acid sites is increased and the selectivity for 2-phenyl isomer decreases from 49.1% to 40.8%. At the same time other isomers are also detected.

Influence of temperature on the alkylation of benzene with 1-octene was studied over a range from 473 to 673 K at a temperature interval of 50 K. The total conversion and selectivity for 2-phenyloctane at various temperatures are shown in Fig. 7. It is seen that at 473 K there is good selectivity for 2-phenyloctane formation

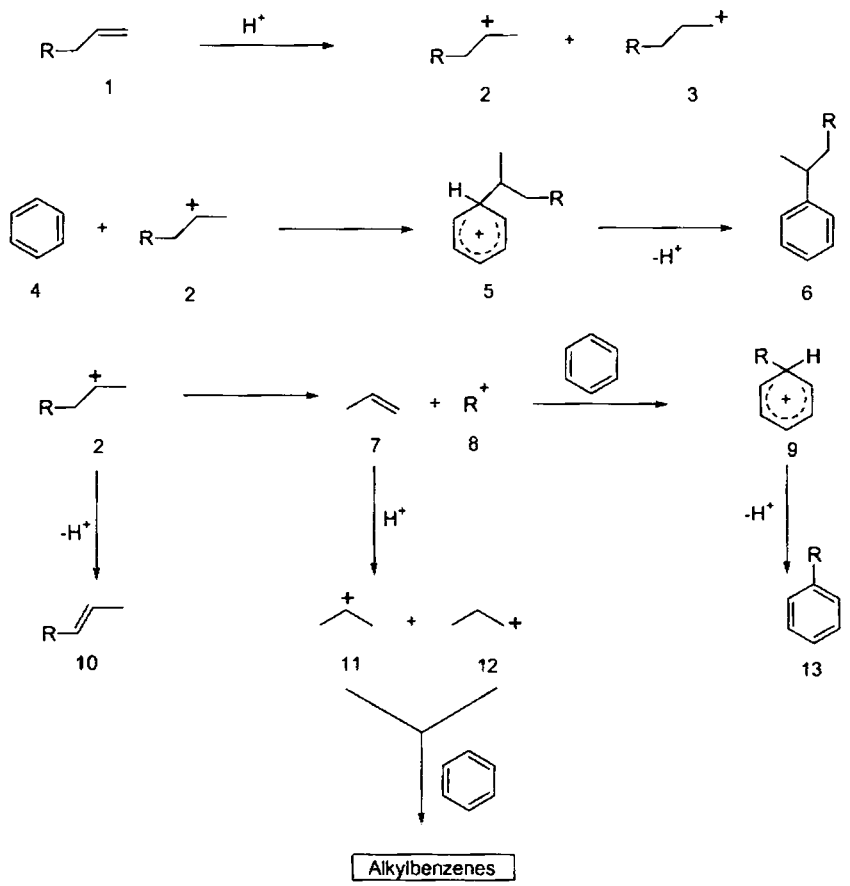

Scheme 1. Alkylation/cracking/isomerization reaction of 1-octene with benzene over zeolite.

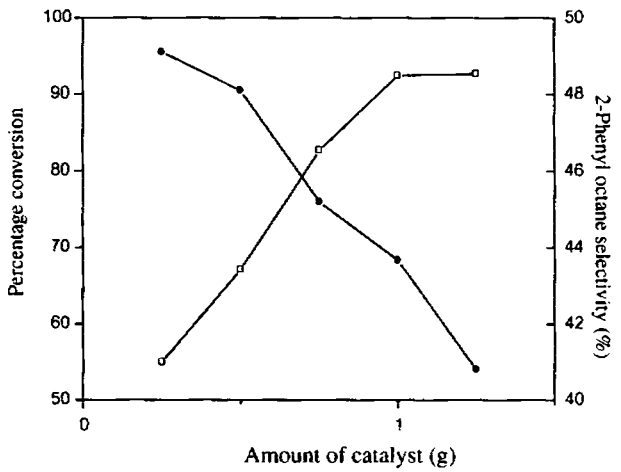

Fig. 6. (●) Selectivity of 2-phenyloctane; (□) 1-octene conversion. Influence of amount of catalyst on the total conversion of 1-octene and selectivity for 2-phenyloctane. Catalyst, H–Y; temperature, 350 °C; weight hour space velocity, 3.43 h^{-1}; benzene to 1-octene molar ratio, 20:1; constant flow of nitrogen, 10 ml/h.

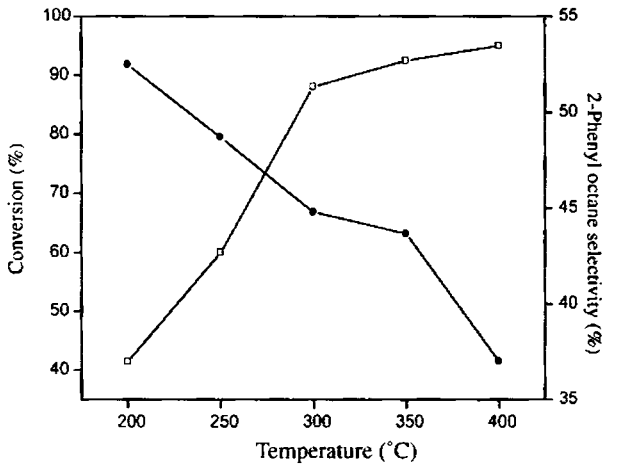

Fig. 7. (●) Selectivity of 2-phenyloctane; (□) conversion of 1-octene. Influence of temperature on the total conversion of 1-octene and selectivity for 2-phenyloctane. Catalyst, H–Y; catalyst amount, 1 g; weight hour space velocity, 3.43 h^{-1}; benzene to 1-octene molar ratio 20:1; constant flow of nitrogen, 10 ml/h.

even though the conversion is low. As the temperature increases from 473 to 673 K, the total conversion increases at the expense of selectivity. This might be due to the increasing probabilities of catalytic cracking, rapid equilibration of the olefin isomer or easy diffusion of the bulkiest LAB isomer out of the zeolite cavities at higher temperature. At 673 K the selectivity was only 37%.

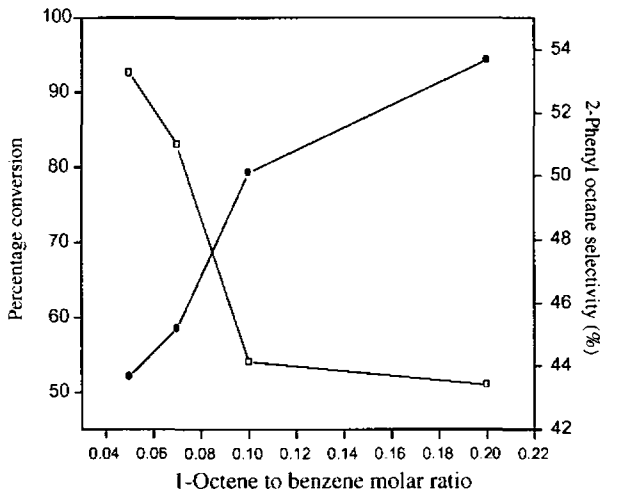

Fig. 8. (□) Selectivity of 2-phenyloctane; (●) conversion of 1-octene. Conversion of 1-octene and selectivity for 2-phenyloctane as a function of molar ratio. Catalyst, H–Y; catalyst amount, 1 g; weight hour space velocity, 3.43 h^{-1}; reaction temperature, 350 °C; constant flow of nitrogen, 10 ml/h.

Molar ratios of the reactants have a marked influence on the rate of a reaction. The reactivity of the catalyst was studied for different molar ratios (solvation effect) and is shown in Fig. 8. There is a drastic increase in the conversion when the molar ratio is increased from 10:1 to 15:1 whereas, the selectivity decreased marginally. As this reversible reaction reaches equilibrium state, an increase in the amount of benzene leads to an increase in conversion of 1-octene. At the same time, the isomerization of 2-phenyloctane to 3-phenyl and 4-phenyl isomer results in a small decrease of the selectivity.

Data on Table 2 shows the variation of conversion and selectivity with change of flow rate (or weight hourly space velocity, h^{-1}). As the flow rate increases from 3 to 5 ml/h (2.57–4.28 h^{-1}) the conversion decreases from 94.6% to 80.9% whereas the selectivity increases from 35.9% to 46.7%. This increase in selectivity might be due to the less time the reactants spend inside the pores of the zeolite, which reduces the chances of isomerization of 2-carbocation to 3 and 4 isomers.

Table 2
Conversion of 1-octene and selectivity for 2-phenyloctane as a function of weight hour space velocity of reactant

Flow rate (ml/h)	Weight hour space velocity (h^{-1})	Percentage conversion	2-Phenyl octane selectivity (%)
3	2.57	90.6	55.90
4	3.43	92.6	53.71
5	4.28	80.9	46.71
6	5.15	79.45	50.54

Catalyst, H–Y; reaction temperature, 350 °C; amount of catalyst, 1 g; 1-octene to benzene molar ratio, 1:20; constant flow of nitrogen, 10 ml/min.

The catalytic activity for the alkylation of benzene with 1-octene over parent and the as-exchanged faujasite–Y forms are shown in Table 3. Binder free Na–Y and K–Y show very low activity and selectivity for the conversion of 1-octene to 2-phenyl isomer. The effect of sodium and potassium ions on the activity of Brönsted type of zeolites in acid catalyzed reactions has been recognized very early especially in the case of faujasite. It was proposed that these residual cations have a poisoning effect on the acidity, i.e., a particular Na^+ or K^+ ion present within the decationated zeolite has a neutralizing effect over a large number of the existing protons [25]. Recently, it has been shown that the effect of residual Na^+ ions was to weaken the Brönsted acid sites, without actually neutralizing more than one Brönsted site per Na^+ ion. Pure as-exchanged Mg–Y showed comparatively good activity and selectivity for 2-phenyloctane over the Na and K forms. Catalytic efficiency follow an order $Mg^{2+} > Na^+ > K^+$ in the pure as well as rare earth modified forms (Table 3). The results

Table 3
Conversion of 1-octene and selectivity for 2-phenyloctane over different zeolite systems

Catalyst system	Flow rate [WHSV] (h^{-1})	Double bond isomerization	Alkene conversion (%)	2-Phenyl octane selectivity (%)	Dialkyl benzenes (%)	Others (%)[a]
Na–Y	3.43	Yes	13.0	40.0	1.6	58.4
H–Y	3.43	Yes	92.6	43.6	2.0	54.4
CeNa–Y	3.43	Yes	81.4	61.0	4.0	35.0
LaNa–Y	3.43	Yes	71.8	56.0	2.1	41.9
K–Y	3.43	Yes	12.5	42.2	1.4	56.4
CeK–Y	3.43	Yes	73.1	60.8	3.6	35.6
LaK–Y	3.43	Yes	65.0	57.5	1.9	40.6
Mg–Y	3.43	Yes	42.3	48.4	2.1	49.5
CeMg–Y	3.43	Yes	84.7	66.7	4.4	28.9
LaMg–Y	3.43	Yes	70.3	58.2	2.5	44.3
H-Mor	3.43	Yes	94.1	74.0	1.4	24.6

Reaction temperature, 350 °C; amount catalyst, 1 g; 1-octene to benzene molar ratio, 1:20; weight hour space velocity, 3.43 ml; constant flow of nitrogen, 10 ml/min.

[a] Others include mainly 3-phenyl and 4-phenybenzenes and trialkylates. Small amounts of other lower hydrocarbons formed during the reaction through cracking, which reacts with benzene to form lower alkyl benzenes.

are consistent with trend of acid strength as measured by NH_3 -TPD (Table 1). This very specific influence of Mg^{2+} cation, which improves the catalytic performance significantly by introducing a high acid strength, is due to its very high polarizing power (small size coupled with greater charge compared to Na^+ or K^+), which affects the OH bond strength through the zeolite lattice. Higher values for the electronegativity of the counter cation according to Sanderson principle create stronger acid sites in the zeolite matrix. A similar explanation is given to increased catalytic activity of CeNa–Y and CeMg–Y. The entire as exchanged zeolites exhibit lower conversion of 1-octene but more selectivity for the formation 2-phenyloctane. Among the different modified forms, CeNa–Y and CeMg–Y shows the maximum conversion and selectivity due to their comparable acidity. Whereas in the case of lanthanum series, LaMg–Y exhibits smaller activity than LaNa–Y. Mg^{2+} with its larger charge induces greater electrostatic repulsive field around La^{3+} cations causing a greater tendency for its migration from the super cages to small cages in the sodalite unit. This produces more inaccessible Brönsted acidity through the hydrolysis of La^{3+} ions in the small cages consequently reducing the total acidity and activity. The decreased activity of potassium forms are attributed to its low acidity value over the corresponding Na or Mg series. The conversion and selectivity for all the systems are consistent with the acidity values from ammonia TPD.

To compare the activity of different as-exchanged zeolite–Y systems with standard catalytic systems, alkylation of benzene with 1-octene was performed over H-mordenite. It shows much high activity and selectivity for this reaction, 94.1% and 74.7%, respectively. This variation in activity is due to their structural difference. HMOR has a bi-directional pore system with parallel circular 12-ring channels (0.65×0.70 nm) and elliptical 8-ring channels (0.26×0.57 nm). However, it practically functions as unidirectional pore system as the 8-ring channels do not allow the passage of the usual molecules whereas H–Y or its modified systems have large cavities (1.3 nm diameter) along with the 3-D pore systems (0.73 nm) [24]. In the case of H-M, shape selectivity appears to play an important role producing maximum 2-phenyl isomer. However, they suffer from very fast deactivation as evident from time on stream studies (not discussed).

5. Deactivation studies

Though zeolites possess very high activity and selectivity for the production of 2-phenyl isomers, they are not very stable, stability being one of the most important qualities for an industrial catalyst. It has been proposed that the deactivation is due to the formation and trapping of heavy alkylate (known as coke) in the pores and cavities of zeolites. Da et al. [40] proposed that the deactivation of large pore zeolites like H-FAU, H-MOR, etc. during the alkylation of toluene with 1-heptene, is due to heptyltoluenes blocked in the pores. Deactivation cannot be completely avoided and regeneration of catalyst by coke removal is inevitable for the industrial application of the catalyst. Generally, coke removal is carried out through oxidative treatment under constant airflow at high temperature. Regeneration temperature has a great effect on the activity of the regenerated catalyst. The product distribution for the deactivated and the regenerated zeolite catalyst is almost identical [41–43].

Alkylation reaction was carried out for 14 h continuously over the H–Y, LaNa–Y and CeNa–Y zeolite catalysts and products were collected at intervals of 2 h. The deactivated catalyst was taken out from the reactor, washed with acetone, dried in the oven at 383 K for overnight. It was then kept in a silica crucible inside the muffle furnace and was then calcined at different temperatures in the range of 423–773 K and at 773 K for 5 h with a heating rate of 12 K/min with a constant air blowing over the sample [44,45]. Carrying out reaction with the regenerated sample we could get a maximum conversion of 91.5% for H–Y, 79.4% for CeNa–Y and 73.8% for LaNa–Y, which are very close to the conversion obtained for the fresh catalysts.

The conversion and selectivity as a function of reaction time for the deactivation studies is shown in Table 4. In the case of H–Y the percentage conversion of 1-octene increases from 2 to 8th hour and then decreases slowly while the selectivity for 2-phenyloctane increases up to 12th hour and then decreases. Maximum selectivity of 57.5% was observed at 12th hour. This observation shows that the zeolite catalysts used have a considerable resistance to deactivation and attains a steady state upon progression of the reaction. The increase in selectivity is due to the blocking of unwanted pores of the catalyst upon coking, which prevents the diffusion of isomerized products like 3 or 4-phenyloctane coming out of the zeolite pores. Here the catalyst deactivation must be due to the olefin polymerization, which is maximum at higher olefin to benzene molar ratio [43]. It is also clear from table that LaNa–Y and CeNa–Y forms exhibits better stability towards reaction conditions than the pure H–Y. CeNa–Y shows a maximum conversion (80%) at the 4th hour and remains almost constant. Whereas the selectivity for the 2-phenyl isomer increases slowly with time and reaches maximum at the 14th hour and this is clearly due to the blocking of unwanted pores of the catalyst upon coking just as in the case of H–Y. It practically prevents the diffusion of isomerized products like 3- or 4-phenyloctane coming out of the zeolite pores. The formation of dialkylate was maximum at 2nd hour (4.5% and 3.4%, respectively, for CeNa–Y and LaNa–Y) and then decreases slowly. This

Table 4
Deactivation of H–Y, CeNa–Y and LaNa–Y during the alkylation reaction

Catalyst system		Time (h)						
		2	4	6	8	10	12	14
H–Y	Conversion for 1-octene (%)	64.0	92.6	92.8	93.2	90.3	84.2	81.1
	Selectivity for 2-phenyloctane (%)	34.5	43.7	51.8	50.7	52.9	57.5	56.7
	Dialkylbenzenes (%)	3.9	3.5	3.2	3.2	2.4	2.3	2.0
CeNa–Y	Conversion for 1-octene (%)	77.3	81.0	80.8	80.4	80.3	79.2	78.9
	Selectivity for 2-phenyloctane (%)	60.5	63.0	63.1	63.9	64.5	64.7	65.9
	Dialkylbenzenes (%)	4.5	4.2	3.9	3.4	3.2	1.7	1.1
LaNa–Y	Conversion for 1-octene (%)	71.9	76.9	72.4	72.2	72.0	71.2	70.4
	Selectivity for 2-phenyloctane (%)	51.5	56.5	56.9	57.6	61.6	61.9	62.3
	Dialkylbenzenes (%)	3.4	2.8	2.0	1.8	1.6	1.6	1.5

Reaction temperature, 350 °C; amount of catalyst,1 g; 1-octene to benzene molar ratio, 1:20; weight hour space velocity, ~3.43 ml; constant flow of nitrogen, 10 ml/h.

decrease in the dialkylate formation is also due to the deposition of coke in the pores, which prevents the diffusion of heavy dialkylate out of the pores. A similar trend is observed in the case of lanthanum-exchanged zeolite also. In this case a maximum conversion of 76.9% is observed at the 4th hour, where as the maximum selectivity of 62.3% was at the 14th hour. The stability towards reaction conditions for the rare earth modified forms over the H–Y is an indication of the improved structural characteristics as evidenced by various physico-chemical studies discussed earlier.

6. Conclusions

Exchange of H–Y with Na, K and Mg cation introduces broadening in the ^{27}Al MAS NMR spectra. This broadening is caused by a distribution of chemical shifts due to aluminium atoms in the locality of strained framework, i.e., due to vicinity of cations, and by aluminium atoms, which are not in the neighborhood of these cations. Lanthanum exchanged forms invariably exhibits migration tendency. Between the three residual cations used, Mg^{2+} execute the greater migration of the lanthanum cations from super cages to the small cages. This is evident from the chemical shift values of ^{29}Si MAS NMR and the moderate acidity values from ammonia TPD studies. Also, lanthanum-exchanged zeolites show low conversion and selectivity for 2-phenyloctane in the alkylation reaction. Exchange of H–Y with Na, K and Mg and subsequently with rare earth cations improves the structural and textural properties of the zeolite. These improvements ultimately result in an increased selectivity for the most desired 2-phenyloctane in the alkylation reaction of benzene with 1-octene. Modification in the structural and textural properties seems to provide a better shape selectivity in the material. A comparison of the selectivity of different as-exchanged zeolites shows that the CeMg–Y produces maximum 2-phenyl isomer. A better selectivity in the case of model H-Mor is due to its rather small pore compared to H–Y and an effective uni-directional pore opening. Deactivation studies show that the rare earth exchanged zeolites show better stability towards reaction conditions.

Acknowledgements

Authors are thankful to Dr. Suriaprakash, Sophisticated Instruments Facility, Indian Institute of Science (IISc), Bangalore for fruitful discussions and providing solid-state NMR results. We are grateful to Dr. Vikramjayaram, Professor, Department of Metallurgy, IISc, Bangalore for providing EDX. B. Thomas thanks Prof. Michael Hunger, Stuttgart University, Germany for helpful suggestions on solid-state NMR studies. Financial support from University Grant Commission, Govt. of India, is gratefully acknowledged.

References

[1] J. Weitkamp, Ind. Eng. Chem. Prod. Es. Rev. 21 (1982) 550.
[2] J.S. Magee, J.J. Balzek, in: J.A.J.A. Rabo (Ed.), Zeolite Chemistry and Catalysis, American Chemical Society, Washington DC, 1976, p. 615.
[3] S. Sivashankar, A. Thangaraj, J. Catal. 138 (1992) 386.
[4] Y. Cao, R. Kessas, C. Naccache, Y.B. Taarit, Appl. Catal. A: Gen. 184 (1999) 231.
[5] C.F. lin, K.-J. Chao, J. Phy. Chem. B 95 (1991) 941.
[6] K.J. Chao, J.Y. Chen, S.H. Chen, P.S. Shy, J. Chem. Soc. Faraday Trans. 86 (18) (1990) 3167.
[7] M. Hunger, G. Engelhardt, J. Weitkamp, Micropor. Mater. 3 (1995) 497.
[8] M. Hunger, G. Engelhardt, H. Koller, J. Weitkamp, Solid State Nucl. Magn. Reson. 2 (1993) 111.
[9] L.B. Welsh, S.L. Lambert, in: W.-E. Flank, T.E. Whyte (Eds.), Perpectives in Molecular Sieve Science, American Chemical Society, Washington DC, 1998, p. 328.
[10] H.K. Bayer, G. Pal-Barbely, H.G. Karge, Mesopor. Mater. 1 (1993) 67.
[11] R. Challoner, R. Harries, Zeolites 11 (1991) 265.

[12] M.T. Melchior, D.E.W. Vaghan, A.J. Jacobson, J. Am. Chem. Soc. 104 (1982) 4859.
[13] S. Hayashi, K. Hayamizu, O. Yamamoto, Bull. Chem. Soc. Jpn. 60 (1987) 105.
[14] J. Klinowski, Chem. Rev. 91 (1991) 1459.
[15] K.J. Chao, J.Y. Chern, J. Phy. Chem. B 93 (1989) 1401.
[16] J.L. Berna, L. Cavalli, C. Renta, Tenside Surf. 32 (2) (1995) 122.
[17] J.H. Clark, G.L. Monks, D.J. Nightingale, P.M. Price, J.F. White, J. Catal. 19 (2000) 348.
[18] C. Hu, Y. Zhang, L. Xu, G. Peng, Appl. Catal. A: Gen. 177 (1999) 237.
[19] J.F. Knifton, P.R. Anantaneni, P.E. Dai, M.E. Stockton, Catal. Lett. 75 (2001) 1–2.
[20] M. Han, Z. Cui, C. Xu, W. Chen, Y. Jin, Appl. Catal. A: Gen. 238 (2003) 99.
[21] Y.B. Young, US Patent, 4301317, 1981.
[22] J.L.G. de Almeida, M. Dufaux, Y.B. Taarit, C. Naccache, Appl. Catal. A: Gen. 114 (1994) 141.
[23] J.F. Knifton, P.R. Anantaneni, US Patent, 5777187, 1998.
[24] B. Wang, W. Lee, T.X. Cai, S.-E. Park, Catal. Lett. 76 (2001) 1.
[25] J.A. Kocal, US Patent, 5196574, 1993.
[26] N.A. Collins, L.A. Green, A.A. Gupte, A.O. Marlen, Tracy, III, J. William, US Patent, 5705724, 1998.
[27] J.F. Knifton, P.R. Anantaneni, P.E. Dai, US Patent, 5847254, 1998.
[28] Y. Cao, R. Kessas, C. Naccacha, Y.B. Taarit, Appl. Catal. A: Gen. 184 (1999) 231.
[29] J.A. Kocal, D.J. Korous, US Patent, 5276231, 1994.
[30] J.A. Kocal, B.V. Vora, T. Imai, Appl. Catal. A: Gen. 221 (2001) 295.
[31] D. Terribile, A. Trovarelli, J. Llorca, C. Deleitenburg, G. Dolectti, J. Catal. 178 (1998) 299.
[32] P. Roessner, K.H. Steinberg, H. Winklert, Zeolites 7 (1987) 47.
[33] S.C. Laha, P. Mukherjee, S.R. Sarkar, R. Kumar, J. Catal. 207 (2002) 213.
[34] G. Engelhardt, H. Koller, P. Sieger, W. Depmeir, A. Samosan, Solid State Nucl. Magn. Reson. 1 (1992) 127.
[35] D. Massiot, C. Bessada, J.P. Coutures, F. Taulelle, J. Magn. Res. 96 (1990) 231.
[36] M. Hunger, U. Scheuk, A. Buchhole, J. Phy. Chem. B 104 (2000) 12230.
[37] R. Szostak, Molecular Sieves—principles of synthesis and identification, Van Nostrand Reinhold catalysis series, 1989, p. 328.
[38] M. Weihe, M. Hunger, M. Breuninger, H.G. Karge, J. Weitkamp, J. Catal. 198 (2001) 256.
[39] A.E. Hirschler, J. Catal. 2 (1963) 428.
[40] Z. Da, P. Magnoux, M. Guinet, Catal. Lett. 61 (1999) 203.
[41] W.G. Liang, Y. Jin, Z. Wang, B. Han, M. He, E. Min, Zeolites 17 (1996) 297.
[42] B.V. Vora, P. R. Cottrell, US Patent, 5012021 1991.
[43] E.E. Wolf, F. Alfani, Catal. Rev. Sci. Eng. 24 (1982) 329.
[44] Z. Da, H. Han, P. Magnoux, M. Guisnet, Appl. Catal. A: Gen. 219 (2001) 45.
[45] S.M. Csicery, Zeolites 7 (1989) 202.